4.2 TROPICAL DENDRITIC CUMULUS: AN OBSERVATIONAL ANALYSIS

Stephen D. Nicholls and George S. Young*

Department of Meteorology, The Pennsylvania State University, University Park, Pennsylvania

1. INTRODUCTION

Analyzing mesoscale cloud formations over the open ocean proved difficult until the 1960's because the available *in situ* observations only provided a patchwork of local views, and as a result there was little insight into mesoscale cloud organization. Thus, with the notable exception of some aircraft studies such as (Malkus and Riehl 1964), little data was available on large mesoscale structures until the first meteorological satellite, Television Infrared Observational Satellite (TIROS), was launched in 1960 and the age of space-borne remote sensing began. TIROS and subsequent meteorological imaging satellites have made it possible to observe mesoscale patterns in what a surface observer would see as merely scattered or broken stratocumulus (Hubert 1966, Agee 1984, Garay et al. 2004, Young and Sikora 2003).

One such unexpected mesoscale pattern that has been observed via satellite is the actinoform (i.e. ray-like starburst) stratocumulus (Hubert 1966, Agee 1984, Garay et al. 2004). These cloud patterns reflect the presence of mesoscale circulations within marine stratocumulus clouds above the cool surface currents of the eastern tropical oceans. An equally striking pattern can, however, be seen in relatively shallow cumulus over warm surface ocean currents elsewhere in the tropics. Under appropriate synoptic conditions (discussed below) the shallow and towering cumulus in these regions can form a compound branching (dendritic) patterns as shown in figures 1, 2, and 3. These dendritic cumulus patterns have not received the attention given by Agee and others to actinoform stratocumulus. Therefore, these cumulus patterns are the focus of the current study.

Tropical dendritic cumulus formations merit study because of both their abundance (1,216 cases observed in our 30 month study period) and their ability to form these patterns within areas of shallow atmospheric convection on a scale ranging from one hundred to a few thousand kilometers. Following the approach taken by Garay et al. (2004) with actinoform stratocumulus, a quantitative study of dendritic cumulus formations is carried out using a combination of satellite imagery and winds supported by large-scale analyses. Tropical dendritic cumulus was observed during a pilot study to be common enough to permit the collection of a large sample, so statistical analysis of the results was undertaken.

This observational study of dendritic cumulus formations used 30 months of data from July 1, 2001 to December 31, 2003. Cases were then collected by examining the 250 m resolution, full-color images from the Moderate-resolution Imaging Spectroradiometer (MODIS; King et al. 1992) instrument aboard the Aeronautic and Space Administration (NASA) Terra and Aqua satellites. The present examination was restricted to those images archived online at the following URL: http://rapidfire.sci.gsfc.nasa.gov/realtime/?calendar. Because a pilot study showed that dendritic cumulus formations occur only over tropical latitudes, the examination of the archives was then further limited to those images taken between 25° N and 25° S. Even with this restriction, the number of images examined was still well in the thousands. Of these, 1,216 included tropical dendritic cumulus formations.

Because full analysis of 1,216 cases was impractical, 61 of these cases were chosen at random (i.e. using a random number generator) for quantitative analysis of both the dendritic cloud formation and the synoptic environment in which it formed. This number was predicated on the requirements for subsequent statistical analysis of the results. As 30 cases are generally considered a minimum for useable averages, it was decided to double the number to assure robustness and add one for good measure. Any sample size on this scale provided a reasonable compromise between analysis effort and statistical robustness. Supporting data were obtained from the multi-spectral MODIS imagery, the NOAA SeaWinds scatterometer aboard the QuikSCAT satellite (Weissman et al. 2002), and the National Centers for Environmental Prediction (NCEP) reanalysis (Kalnay et al. 1996). The 3-6-7-band cloud phase product of the MODIS multi-spectral data (King et al. 1992, 1997) was used to check the cloud depth and height. Ice-free clouds, depicted by reddish shading, were assumed to be shallow or towering cumulus rather than deep cumulonimbus (Johnson et al. 1999). The NCEP reanalysis provided profiles of vector wind, temperature and stability for the lower troposphere along with the information required to calculate lower tropospheric temperature advection. The reanalysis surface

---

* *Corresponding author address:* George S. Young, Dept. of Meteorology, 503 Walker Building, University Park PA, 16802; e-mail: young@meteo.psu.edu

winds were then verified by comparison with the corresponding QuikSCAT observations.

2. PROCEDURES

a. Dendritic Cumulus Formation Geometry

Each of the archived MODIS images spans an area of 15° of longitude by 20° of latitude and is tilted counter-clockwise by 10° from a north-south alignment because of the orbit inclination of the MODIS satellites in the tropics. This image information was used to estimate the area covered by each dendritic cumulus formation and to correct the cloud-pattern alignment angles to correspond to standard meteorological coordinates. Because the archived MODIS images are distorted near their cross-track edges, only data from the central portion of the images were analyzed. The dendrite alignment angle is defined here as the direction towards which the stems of the Y-shaped elements point. The alignment of the numerous Y-elements in each dendrite was subjectively analyzed and averaged prior to quantitative measurement of the angle for each of the 61 cases. The geographic location of the estimated center of each dendritic cumulus formation and the area covered by the formation were also recorded. The alignment angles were recorded in degrees from true north, the locations in decimal degrees of latitude and longitude, and the area in square kilometers. These data were analyzed, as described below, to determine the geographic regions in which dendritic cumulus patterns form, the synoptic setting required for their development, and the relationship between their orientation and the synoptic scale winds.

b. Synoptic Environmental Data

To determine the synoptic environment associated with a lower-tropospheric oceanic convective system, the winds, sea and air temperatures and atmospheric stability are required (e.g. Woodcock 1940, 1975, Young et al. 2002). Because of the worldwide distribution of dendritic cumulus formations over the tropics, synoptic wind data were acquired from the QuikSCAT satellite-borne scatterometer and NCEP reanalysis data set. The NCEP reanalysis was selected because of both its global coverage and its 2.5° resolution yielded grid cells of area similar that of tropical dendritic cumulus formations. The scatterometer data had a much higher 25 km resolution, which was more than was required to ascertain the synoptic setting. The scatterometer data were primarily used to verify the reanalysis surface winds. The reanalysis dataset provided sea surface and air temperatures as well as wind vectors at the surface, 850 mb and 700 mb. Differences between these pressure levels were used to assess layer stability and shear vectors at the location of each sampled dendritic cumulus formation. The combination of wind and temperature patterns was used to assess temperature advection at the three lower tropospheric levels.

3. RESULTS

a. Dendritic Cumulus Formations

Tropical dendritic cumulus formations exhibit a compound branching, fractal-like structure of shallow and towering cumulus. Closer inspection of the 61 individual cases reveals however that the cumulus coverage between the dendrite samples varies considerably. In some cases the individual cumulus clouds are widely scattered except where they form part of the dendritic pattern (Fig 3), while in other cases small cumulus form a more uniform background between branches of the dendritic pattern (Fig 1). Figure 2 shows an intermediate case with patches of scattered cumulus embedded within the dendritic cumulus pattern. Within the 1,216 cased observed in this present study, examples from all parts of this spectrum were common. A histogram of cloud fraction was not computed however, because quantification of coverage by such small clouds is extremely subjective and sensitive to the MODIS satellite image resolution. The MODIS imagery at 250 m resolution is nonetheless sufficient to conclude that dendritic cumulus patterns are a scattered cumulus phenomenon and not one involving broken cumulus or stratocumulus.

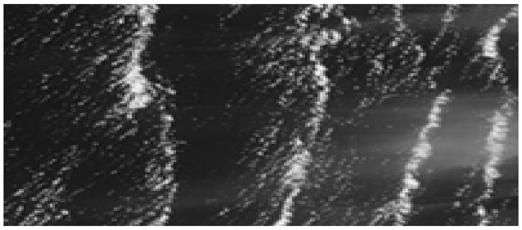

Figure 1: MODIS image of a tropical dendritic cumulus formation embedded in a field of fair-weather cumulus over the western Indian Ocean on September 28, 2004.

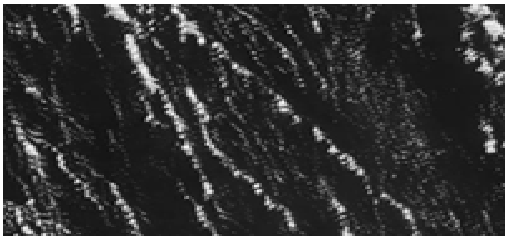

Figure 2: MODIS image of a tropical dendritic cumulus formation with patchy fair-weather cumulus over the southeastern Atlantic Ocean on April 16, 2003.

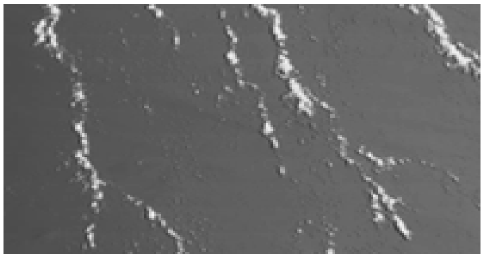

Figure 3: MODIS image of a tropical dendritic cumulus formation with widely scattered fair-weather cumulus between the cloud lines. The image was taken over the western Indian Ocean on September 15, 2001.

b. Geography and Extent

Figure 4 maps the locations where each of the 61 randomly sampled dendritic cumulus formations occurred. All of these formations occurred over warm tropical ocean currents, with distinct gaps in their distribution apparent over the cold Peru Current, and over the warm waters of the western equatorial Pacific and the North Atlantic tropics. These gaps suggest the existence of two constraints on their global distribution. First, cumulus are much less common than stratocumulus over cold tropical currents (Garay et al. 2004), explaining the scarcity of dendritic cumulus formations over the Peru Current. Second, deep precipitating convection is frequent over the warm equatorial western Pacific and along the Inter-Tropical Convergence Zone (ITCZ) in the North Atlantic tropics. Thus, an abundance of deep convection also appears to disrupt mesoscale dendritic organization among shallow cumulus.

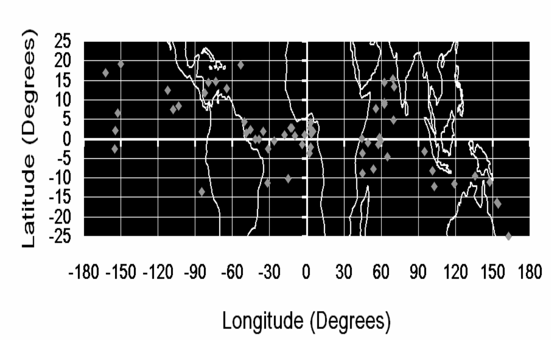

Figure 4: A map depicting the location of each center of the 61 dendritic cumulus formations studied.

c. Temperature and Instability

Both the sea surface temperature and the lower tropospheric air temperature profiles play pivotal roles in causing tropical dendritic cumulus formations to occur, which might be expected from the association of shallow and towering tropical cumulus with lower tropospheric conditional instability. A sea surface temperature (SST) threshold is noticeable within the study sample, because all sample dendrite cases occurred with values of at least 24°C. This SST requirement goes a long way towards explaining why dendritic cumulus formations typically form only between 25°N and 25°S. A shallow layer of conditional instability was also usually present as shown in Table 1. The mean lapse rate in the surface to 850 mb layer is 6.06°C km^{-1}, conditionally unstable, while the mean lapse rate in the 850 to 700 mb layer is 5.32°C km^{-1}, stable. Thus, shallow convection is favored over deep, which keeps with previous the MODIS observations.

	SST	Suface	850 mb	700 mb
Average	27.5	25.8	16.7	8.72
Maximum	24.0	16.8	8.50	6.50
Minimum	30.5	28.5	19.5	10.0

Table 1: NCAR / NCEP derived air and sea surface temperatures at different heights associated with the sixty-one studied sample dendrites.

d. Triggering Mechanisms

Of particular interest for any convective pattern are its triggering mechanisms (Young and Sikora 2003). Because dendritic cumulus formations are comprised of locally enhanced lines of shallow cumulus convection, it was hypothesized that they might be either a precursor or a remnant of a mesoscale area of deep convection. To test this hypothesis the presence or absence of deep convection preceding or succeeding each of the 61 sample images was noted by a human analyst. The result of this analysis was that deep convection was observed in only 25 of the 61 samples the day before and 22 of 61 samples the day after. These results suggest that the deep convective instability is not a prerequisite or result of dendritic cumulus formation. Thus, we need to look further for a trigger mechanism.

The next hypothesis examined was that low-level temperature advection on day of the event might play a role in creating the shallow layer of conditional instability necessary for their formation and dominance over other convective modes. Through analysis of the NCEP reanalysis data it was discovered that surface cold advection was present in varying degrees in 97% (i.e. all but 2) of the 61 sample cases. This finding provides some explanation as to why dendritic cumulus formations do not occur everywhere the SST exceeds 24°C. Moreover, this low-level cold advection requirement sets them apart from the narrow mode linear cloud streets commonly reported over warm tropical oceans (LeMone 1976, Young et al. 2002).

e. Terminating Mechanisms

Equally important for tropical dendritic cumulus formations is the termination mechanism. The environmental factors leading to termination of each of the 61 sample cases were examined using a combination of MODIS imagery and NCEP reanalysis data. For these cases the downwind edge of the dendritic cumulus formation was usually defined by one of five phenomena: a land breeze front, a coast, the onset of warm or neutral temperature advection at the surface, the edge of a cold current, or the boundary of an area of deep convection. The most common termination mechanism for these clouds is an area of deep convection such as a mesoscale convective complex or the ITCZ. The second most common is advection of the cloud formation over an area of cooler water. Conversely, land breeze fronts were the least common cause of dendrite termination because most of the sample dendritic cumulus formations occurred in the open sea with only a handful near the coasts of western Africa and northeastern South America.

f. Wind Speed and Direction

As with linear cloud streets (LeMone 1976, Young et al. 2002), the surface wind and lower-tropospheric shear vectors have a great influence on the alignment of tropical dendritic cumulus patterns. The dependence of alignment on surface wind direction can be seen in figure 5, which, somewhat surprisingly, shows two modes of alignment, one aligned with the surface wind and the other against it. A bimodal distribution such as this is expected with linear cloud streets because their symmetry yields a 180° ambiguity in their alignment. But dendritic cumulus formations have an unambiguous orientation, because the Y-stem points along their alignment axis and the Y-prongs point in the other direction. From figure 6 it can be seen that the Y-stem points either with or against the surface wind with deviations rarely exceeding 30°. Indeed the standard deviation of the sample cases around these two directions is 14.3° about the 0° alignment and 15.6° about the 180° alignment, about what Young et al. (2002) report for the scatter in wind-relative alignment of linear cloud streets. The key question why this bimodal distribution of wind-relative alignment exists is addressed in section 3g.

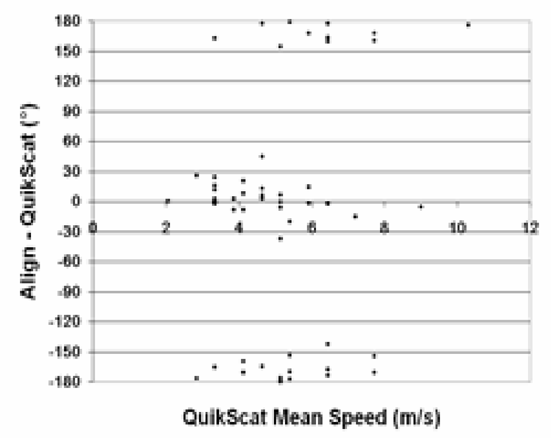

Figure 5: Alignment dependence to the mean wind direction of tropical dendrites to the background wind speed

Figure 6: Tropical dendritic cumulus clouds with a background wind speed of 5.14 m/s. MODIS image from the western Indian Ocean on September 28, 2004.

Another key result shown in figure 5 is the role of wind speed in determining the alignment of a dendritic cumulus formation. This relationship is best illustrated in figure 5 by the dramatic decrease in scatter about both modes of alignment as wind speed increases, which could indicate one of two things. First, it is possible that the reanalysis wind directions have a higher degree of accuracy at higher wind speeds, which is not unreasonable if the magnitude of the vector error does not increase as rapidly as wind speed. Indeed, unless calms are perfectly analyzed, the wind direction error must reach a maximum at zero wind speed. Second, it is possible that whatever process links wind direction to dendrite alignment becomes more effective as wind speed increases. The scatterometer wind directions are highly correlated ($r^2 = 0.55$) with the reanalysis surface wind directions, but are not themselves reliable at very low wind speeds and as a result, the first possibility cannot be tested conclusively. Linear cloud street studies such as LeMone (1976) and Weckwerth et al. (1997), show that wind-alignment of cumulus requires that the wind speed exceed a minimum value (albeit stability-dependent; Weckwerth et al. 1999), giving some support to the second possibility. A broad domain large eddy simulation of moist convection might be required to fully resolve this issue.

The relationship between dendritic cumulus formations and linear cloud streets is clarified somewhat by the wind speed limits in which the two phenomena are observed. While linear cloud streets typically require at least 3 ms^{-1} of surface wind (Weckwerth et al. 1997), dendritic cumulus formations have been observed at speeds ranging from slightly more than 1.5 ms^{-1} to just below 13 ms^{-1}. This wind speed range encompasses the previously reported thresholds for linear cloud streets. Thus, dendritic cumulus formations appear to represent a middle ground between these streets and the random cumulus that occur at lower wind speeds. This finding raises the question of why such a middle ground exists for SST values greater than 24°C but has not been observed under other conditions. The next section will address this issue while resolving the alignment ambiguity mentioned above.

Figure 7: Tropical dendritic cumulus clouds with a background wind speed of 6.69 m/s. MODIS image from the western Timor Sea on November 5, 2001.

The relationship between wind speed and branching angle of the Y-prongs shown in figures 6, 7 and 8 suggests that a gradual transition may take place from dendritic cumulus formations to linear cloud streets as wind speed increases. In an effort to quantify this hypothetical relationship the typical branching angle each of the sample images was calculated by first thresholding the image to obtain a cumulus mask and then applying the linear feature alignment algorithm of Carbone et al. (2002) to the mask. This objective method, adapted from the Hovmoller diagram feature-tracking application, works imperfectly on a discontinuous cumulus field, but is superior to subjective estimates of the typical spread angle in a complex cloud field. A successful analysis was accomplished on 40 of the 61 sample cases, providing mean cloud-line alignment angles that agreed well with the subjective analysis. The standard deviation of these cloud-line alignment angles was used as a proxy for the average branching angle of each dendritic cumulus formation. Any correlation between this proxy and the surface wind speed was negligible however, providing no support to the hypothesis of a gradual transition from dendrites to cloud streets. A possible explanation for this scatter, in terms of a dependence on both convective intensity and wind shear magnitude is provided as a consequence of the dendrite formation mechanism hypothesized and discussed in the next section.

Figure 8: Tropical dendritic cumulus clouds with a background wind speed of 10.29 m/s. MODIS image from offshore of Tanzania on September 25, 2001.

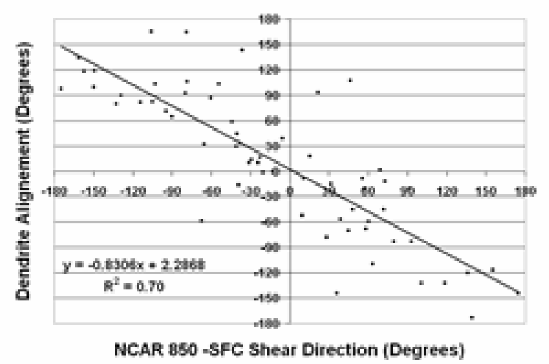

Figure 9: Alignment dependence of dendrites to wind shear from 850 mb to the surface.

g. Shear Influence and Branch Structure

To explain the bimodal relationship between the surface wind direction and alignment of tropical dendritic cumulus formations it is necessary to turn to the lower tropospheric shear. In contrast to the situation for linear cloud streets, where the boundary layer shear and the surface wind are usually in roughly the same direction (e.g. Weckwerth et al. 1997, 1999, Young et al. 2002), these two vectors are equally likely to oppose each other in dendritic cumulus formations. In 41 of the 61 sample dendrite cases the surface to 850 mb shear vector was opposed to rather than aligned with the surface wind.

Thus, shear and alignment both have a bimodal distribution about the surface wind direction for dendritic cumulus formations. This difference between dendritic cumulus formations and linear cloud streets suggests that the orientation of the boundary layer shear may determine the branching alignment of the dendritic pattern. Figure 9 confirms this hypothesis, indicating a strong linear relationship between the two parameters ($r^2 = 0.70$). This correlation can be improved further, to $r^2 = 0.96$, by using the surface to 850 mb shear merely to resolve the bimodal relationship between surface wind direction and dendrite alignment. By using the reverse of the wind direction in those cases where it is more closely aligned to the shear, the bimodal relationship is collapsed, resolving this directional ambiguity. Figure 10 displays the relationship of dendrite alignment to this new direction parameter. Thus, while the individual Y-elements of dendritic cumulus formations themselves align closer with the surface wind than with the surface to 850 mb shear, they assume an orientation along the surface wind direction such that the Y-prongs point down shear. A regression line between the resulting prediction and the observed alignment has a slope of 0.96 and an intercept of 8.1° suggesting that there is very little multiplicative or additive bias.

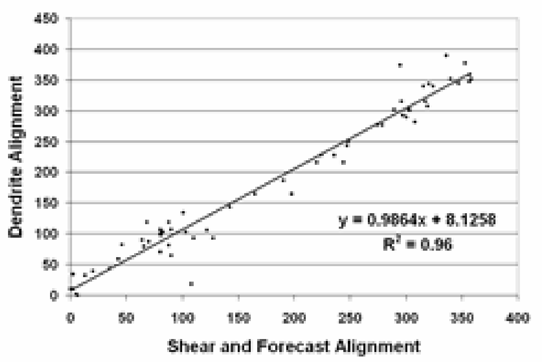

Figure 10: Dendrite alignment dependence on surface wind direction after shear-based correction and folding to 0-360 range.

One explanation for this shear dependent alignment lies in the superposition of synoptic-scale shear and the secondary circulations generated by the individual cumulus lines. If these secondary circulations are strong enough they can result in significant variations in the boundary layer shear vector from one side of the cloud line to the other as shown in figure 11. Weaker cloud lines forming near these stronger lines would thus experience divergent shear vectors, angling outward from that line. If these cloud lines are shear-aligned in the manner of linear cloud streets, they would angle out from the original cloud line with the open end of the resulting branching structure oriented down the synoptic shear as shown in figure 12.

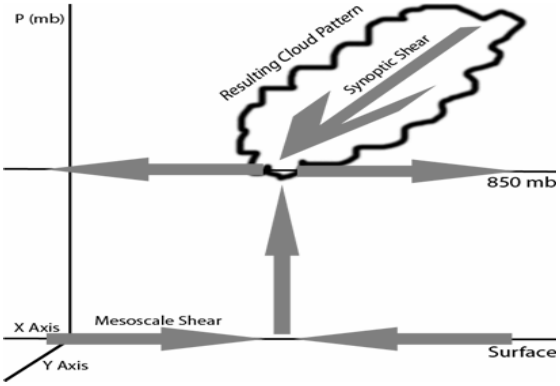

Figure 11: Combined mesoscale shear image of the surface and 850 mb layer.

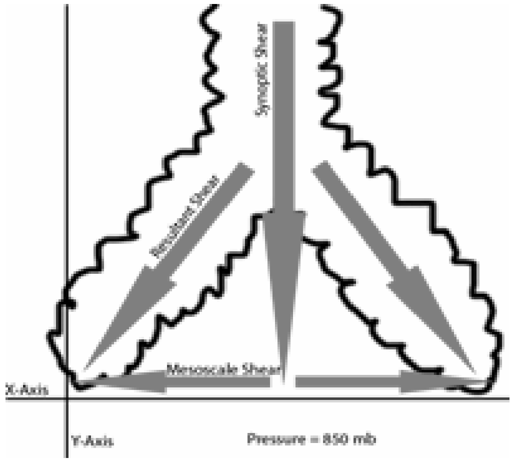

Figure 12: Synoptic and Mesoscale Shear relationship at 850 mb creating dendrite spread seen from above.

This hypothetical explanation raises the question of why, in those synoptic situations where tropical dendritic cumulus formations occur, some cloud lines appear stronger, and thus more shear controlling, than others. One possible explanation is the noticeable increase in stability between the surface to 850 and the 850 to 700 mb layers. The stronger cloud lines in a dendritic cumulus formation are often composed of greater amounts of towering cumulus, while the weaker cloud lines are composed of shallow cumulus mediocris and humulus. Towering cumulus lines use this stability gradient to their own advantage by lifting it locally while lowering it on either side as shown in figure 13. Thus, cumulus lines forming adjacent to pre-existing towering cumulus lines would develop in a shallower layer of conditionally unstable air as well within the modified shear described above. Thus, they will be smaller in size and scope than the stronger cloud lines. A similar pattern of stability modification has been described in the context of deep precipitating convection (Mapes 1993). A broad domain large eddy simulation of moist convection might be used to test the applicability of this mechanism to tropical dendritic cumulus formations.

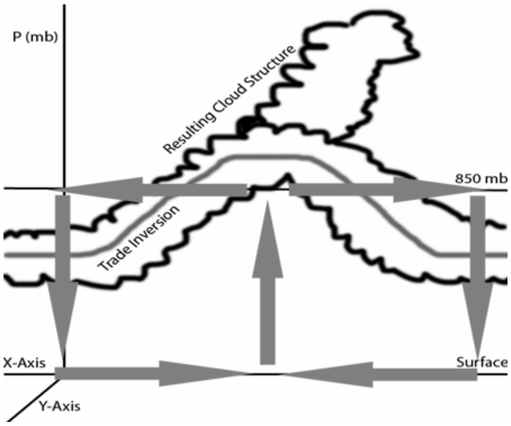

Figure 13: Suppression of trade inversion by mesoscale shearing flow at 850 mb and the surface.

These arguments suggest that linear elements of dendritic cumulus formations differ from linear cloud streets in that their secondary circulations can modify the background wind and stability profiles experienced by neighboring cloud lines. Thus, they would be favored when synoptic shear is not overwhelmingly stronger than the shear produced by the secondary circulations of the deepest cloud lines and when these cloud lines and their secondary circulations penetrated up into a layer of increased stability.

These arguments suggest that linear elements of dendritic cumulus formations differ from linear cloud streets in that their secondary circulations can modify the background wind and stability profiles experienced by neighboring cloud lines that develop later. Thus, they would be favored when synoptic shear is not overwhelmingly more powerful than the shear produced by the secondary circulations of the deepest cloud lines and when these cloud lines and their secondary circulations penetrated up into a layer of increased stability.

4. CONCLUSIONS

This paper documents the frequent occurrence of branching Y-element patterns within fields of shallow and towering cumulus, christened tropical dendritic cumulus formations. These formations occur over warm water tropical oceans (SST > 24°C) with light to moderate winds (1.5 to 13 ms^{-1}). An additional condition for their existence is that some degree of cold air advection must be present at the surface. The combination of cold air advection and warm sea surface favors boundary layer convection as, for example, in cold air outbreaks at higher latitudes. The resulting thermodynamic profile is conditionally unstable in the surface to 850 mb layer, and then stable higher up in the 850 to 700 mb layer. Thus, dendritic cumulus formations occur over tropical waters that are favorable for deep precipitating convection but where synoptic situations which are unfavorable to it. Temporal analysis supports this result as dendritic cumulus formations are neither reliable precursors for areas of deep precipitating convection nor the reverse. As a result, the geographic distribution of tropical dendritic cumulus formations avoids those regions where synoptic forcing favors deep convection (e.g. the warm pool of the western equatorial Pacific and the Atlantic ITCZ).

Dendritic cumulus formations align with both the surface wind and surface to 850 mb shear vector, much as do linear cloud streets. Yet the cloud lines in dendritic formations branch frequently while those in conventional cloud street patterns do not typically branch. This difference is hypothesized to result from the formation mechanism of the branching structure itself, the interaction of the secondary circulation of towering cumulus lines with the shear and stability profiles of their surroundings. By locally modifying the shear vector and decreasing the depth of the conditionally unstable layer, this secondary circulation would create conditions favoring shallower cumulus lines branching at a shallow angle from the pre-existing line. This pattern is indeed observed with dendritic cumulus formations. Moreover the alignment and orientation suggested by this mechanism is a good predictor for the observed dendritic structures. Future work should test this secondary circulation hypothesis using a broad domain large eddy simulation of moist convection.

Acknowledgements: This work was supported in part by the Office of Naval Research under grant N00014-04-10539.

5. REFERENCES

Agee, E. M., 1984: Observations from space and thermal convection: A historical perspective. *Bull. Amer. Meteor. Soc*., **65**, 938-949.

Carbone, R. E., J. D. Tuttle, D. A. Ahijevych, and S. B. Trier, 2002: Inferences of predictability associated with warm season precipitation features. *J. Atmos. Sci.*, **59**, 2033-2056.

Garay, M. J., R. Davies, C. Averill, and J. A. Westphal, 2004: Actinoform clouds: Overlooked examples of cloud self-organization at the mesoscale. *Bull. Amer. Meteor. Soc*., **85**, 1585-1594.

Hubert, L. F., 1966: Mesoscale cellular convection. U.S. Department of Commerce, Environmental

Science Services Administration, Meteorological Satellite Laboratory Tech. Rep. 37, 68 pp.

Johnson, R. H., T. M. Rickenbach, S. A. Rutledge, P. E. Ciesielski and W. H. Schubert, 1999: Trimodal characteristics of tropical convection. *J. Climate,* **12**, 397–2418.

Kalnay, E., and Coauthors, 1996: The NCEP/NCAR 40-year reanalysis project. *Bull. Amer. Meteor. Soc*. **77**, 437–471.

King, M. D., Y. J. Kaufman, W. P. Menzel, and D. Tanre, 1992: Remote-sensing of cloud, aerosol, and water-vapor properties from the Moderate Resolution Imaging Spectrometer (MODIS). *IEEE Trans. Geosci. Remote Sens.*, **30**, 2–27.

King, M. D., S.-C. Tsay, S. E. Platnick, M. Wang, and K. N. Liou, 1997: Cloud retrieval algorithms for MODIS: Optical thickness, effective particle radius, and thermodynamic phase. Algorithm Theoretical Basis Documents (ATBD), MODIS Science Team.

LeMone, M. A.. 1976: Modulation of Turbulence Energy by Longitudinal Rolls in an Unstable Planetary Boundary Layer**.** *J. Atmos. Sci.,* **33**, 1308–1320.

Mapes, B. E., 1993: Gregarious tropical convection. *J. Atmos. Sci.*. **50**, 2026–2037.

Malkus, J. S., and H. Riehl, 1964: Cloud structure and distributions over the Tropical Pacific Ocean. *Tellus,* **16,** 275–287.

Weckwerth, T. M., J. W. Wilson, R. M. Wakimoto, 1997: Horizontal convective rolls: Determining the environmental conditions supporting their existence and characteristics. *Mon. Wea. Rev*., 125, 505-526.

Weckwerth, T. M., T. W. Horst, and J. W. Wilson, 1999: An observational study of the evolution of horizontal convective rolls. *Mon. Wea. Rev.*, **127**, 2160-2179.

Weissman, D. E., M. A. Bourassa, and J. Tongue, 2002: Effects of rain rate and wind magnitude on SeaWinds scatterometer wind speed errors. *J. Atmos. Oceanic Technol.,* **19,** 738–746.

Woodcock, A. H., 1940: Convection and soaring over the open sea. *J. Marine. Res*., 3, 248-253.

Woodcock, A. H., 1975: Thermals over the sea and gull flight behavior. *Boundary Layer Met.,* **9**, 63-68.

Young, G. S., D. A. R. Kristovich, M. R. Hjelmfelt, R. C. Foster, 2002: Rolls, streets, waves, and more: A review of quasi-two dimensional structures in the atmospheric boundary layer. *Bull. Amer. Metero. Soc*., **83**, 997-1001. Also, an extended electronic supplement.

Young, G. S., and T. D. Sikora, 2003: Mesoscale stratocumulus bands caused by Gulf Stream meanders. *Mon. Wea. Rev.*, **131**, 2177–2191.